

# Electronic structures and ferromagnetism in transition metals codoped ZnO

Min Sik Park and B. I. Min

*Department of Physics and electron Spin Science Center,  
Pohang University of Science and Technology, Pohang 790-784, Korea*

(Dated: November 10, 2018)

We have investigated electronic structures and magnetic properties of potential ZnO based diluted magnetic semiconductors: (Fe, Co) and (Fe, Cu) codoped ZnO. The origins of ferromagnetism are shown to be different between two. (Fe, Co) codoped ZnO does not have a tendency of Fe-O-Co ferromagnetic cluster formation, and so the double exchange mechanism will not be effective. In contrast, (Fe, Cu) codoped ZnO has a tendency of the Fe-O-Cu ferromagnetic cluster formation with the charge transfer between Fe and Cu, which would lead to the ferromagnetism through the double-exchange mechanism. The ferromagnetic and nearly half-metallic ground state is obtained for (Fe, Cu) codoped ZnO.

PACS numbers: 75.50.Pp, 71.22.+i, 75.50.Dd

## I. INTRODUCTION

Electronics utilizing the spin degree of freedom of electrons, namely “spintronics”, becomes an important emerging field. The spintronics is expected to overcome the limits of traditional microelectronics, such as non-volatility, data processing speed, electric power consumption, and integration densities<sup>1</sup>. Diluted magnetic semiconductors (DMSs) will play a core role in spintronics as semiconductors do in electronics due to easy integration into existing electronic devices. Two types of DMS families have been well studied: II-VI type such as Mn-doped CdTe and ZnSe<sup>2</sup>, and III-V type such as Mn-doped GaAs<sup>3</sup>. In particular, the latter attracts great attention, because it becomes a ferromagnetic (FM) DMS having the Curie temperature  $T_C \sim 110K$ . Recent research effort has been focused on developing a new FM-DMS operating at room temperature<sup>4,5,6,7,8,9</sup>.

Along this line, attempts have been made to fabricate ZnO based DMS. ZnO is a wide-gap ( $E_g \sim 3.44eV$ ) II-VI semiconductor, and so it can be used for ultraviolet light emitting devices. Jin *et al.*<sup>10</sup> fabricated 3d transition metal (TM) doped epitaxial ZnO thin films using the combinatorial laser molecular-beam epitaxy method. However, they have not detected any indication of ferromagnetism. In contrast, Ueda *et al.*<sup>11</sup> observed the FM behaviors in some of the Co-doped ZnO films made by using the pulsed-laser deposition technique with  $T_C$  higher than the room temperature. The reproducibility, however, was less than 10%. Hence the realization of the FM long range order in Co-doped ZnO films is controversial.

On the other hand, there were also trials to make ZnO based DMS by co-doping two TM elements: (Fe,Co) or (Fe,Cu).  $Zn_{1-x}(Co_{0.5}Fe_{0.5})_xO$  films were fabricated by using the reactive magnetron co-sputtering technique<sup>12</sup>, which seemed to have the single phase of the same wurtzite structure as pure ZnO up to  $x=0.15$ . The room temperature ferromagnetism was observed and the rapid thermal annealing under vacuum leads to increases in  $T_C$ , magnetization, and the carrier concentration. Also Cu-doped  $Zn_{1-x}Fe_xO$  bulk samples were fabricated<sup>13</sup>. The

bulk sample has the advantage of insensitivity to the detailed process conditions, over the film sample fabricated under the nonequilibrium condition. They observed the FM behaviors with  $T_C \sim 550K$  and the saturation magnetic moment of  $0.75\mu_B$  per Fe in  $Zn_{0.94}Fe_{0.05}Cu_{0.01}O$ . The saturation magnetic moment increases, as the Cu doping ratio increases up to 1%. In addition, the large magnetoresistance was observed below 100K.

Motivated by these reports of ferromagnetism in TM codoped ZnO, we have studied electronic structures and magnetic properties of (Fe, Co) and (Fe, Cu) codoped ZnO:  $Zn_{0.875}(Fe_{0.5}M_{0.5})_{0.125}O$  ( $M=Co$  or  $Cu$ ). We have used the linearized muffin-tin orbital (LMTO) band method in the local spin-density approximation (LSDA). To explore the Coulomb correlation and the spin-orbit (SO) effect in TM-doped ZnO, we have also employed the LSDA+ $U$ (+SO) method incorporating the Coulomb correlation interaction  $U$  and the SO interaction<sup>14</sup>. ZnO has the wurtzite structure in which anions and cations form hexagonal close-packed lattices. The wurtzite ZnO is composed of tetrahedrons formed by four O anions. For  $Zn_{0.875}(Fe_{0.5}M_{0.5})_{0.125}O$ , we have considered an orthorhombic supercell containing sixteen formula units in the primitive unit cell by replacing two Zn atoms by Fe and  $M$  atoms ( $Zn_{14}Fe_1M_1O_{16}$ ). For the lattice constants, we assumed those of pure ZnO with  $a = 6.4998, b = 11.2580, c = 5.2066 \text{ \AA}$ .

## II. ZnO, Fe- and Co-doped ZnO

First, we have checked the electronic structure of pure wurtzite ZnO without doping elements. The overall band structure of the present LMTO result is consistent with existing results<sup>15,16,17</sup>. As usual in the LSDA calculations, the obtained energy gap  $\sim 0.7 eV$  is only about 20% of the experimental value. Also the position of Zn 3d band ( $-3.0 \sim -5.0 eV$  with respect to the valence band top) is much shallower than the Zn 3d spectrum obtained by photoemission experiment ( $\sim -9.0 eV$ )<sup>18</sup>. The LSDA+ $U$  band method improves the results of LSDA,

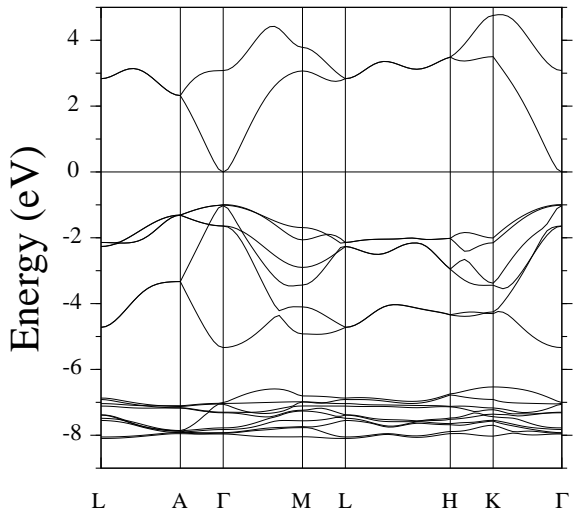


FIG. 1: The LSDA+ $U$  band structure of ZnO with  $U=3.0\text{eV}$  for Zn 3d electrons. The lowest and intermediate bands correspond to mainly Zn 3d and O 2p bands, respectively. Zn 3d bands in the LSDA are too shallow to become mixed with O 2p bands.

but not so satisfactorily. As shown in Fig. 1, the energy gap is increased to  $\sim 1.0\text{ eV}$ , and the position of Zn 3d band becomes deeper ( $-6.0 \sim -7.0\text{ eV}$ ). The LSDA+ $U$  result for Zn 3d position is consistent with result obtained by the GW band calculation<sup>16,17</sup>. Still the energy gap and Zn 3d position are smaller and shallower than experimental values.

We then have performed the LSDA band calculations for single TM-element doped ZnO: Fe- and Co-doped ZnO with 6.25% concentration of TM element. Due to heavy computational load, we have not considered the Coulomb correlation  $U$  for Zn 3d electrons in the supercell calculations of doped ZnO systems<sup>19</sup>. Note that electronic structures of TM doped ZnO have already been reported for 25% concentration of TM element by using the Korringa-Kohn-Rostoker band method combined with the coherent potential approximation<sup>5</sup>. They found that V-, Cr-, Fe-, Co-, and Ni-doped ZnO would have the FM ground states rather than the spin-glass states. With this background, we thus consider below only the FM states for Fe-, and Co-doped ZnO with more realistic TM doping concentration.

Figure 2 shows the LSDA total density of states (DOS) and TM 3d projected local DOS (PLDOS) for  $\text{Zn}_{1-x}\text{Fe}_x\text{O}$  and those for  $\text{Zn}_{1-x}\text{Co}_x\text{O}$  ( $x = 0.0625$ ). For both Fe- and Co-doped ZnO, we have obtained nearly *half-metallic* electronic structures, that is, the conduction electrons at the Fermi level  $E_F$  are almost 100% spin polarized. The minority spin 3d states of both Fe and Co near  $E_F$  are seen to be hybridized slightly with the conduction band (see Fig. 3). Both for Fe-doped and Co-doped ZnO, the

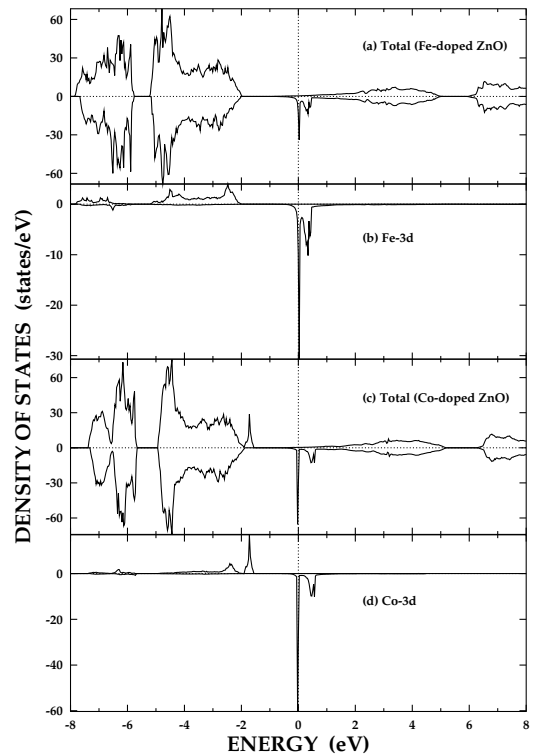


FIG. 2: The LSDA total and TM 3d PLDOSs of  $\text{Zn}_{0.9375}\text{Fe}_{0.0625}\text{O}$  and  $\text{Zn}_{0.9375}\text{Co}_{0.0625}\text{O}$ .

Fermi level cuts the sharp minority spin  $e_g$  states. Note that Fe and Co are located at tetrahedral centers formed by O ions, and so  $e_g$  states are lower in energy than  $t_{2g}$  states. Since there is nearly one more  $d$ -electron in Co-doped ZnO, the Fermi level is located near the valley between Co  $e_g$  and  $t_{2g}$  minority spin state. The exchange splittings are larger than the crystal field splittings, reflecting high spin states of Fe and Co in ZnO. Especially, the exchange splitting in Fe-doped ZnO is very large to locate both  $e_g$  and  $t_{2g}$  states deep in energy, and so the majority spin Fe  $t_{2g}$  states become fully hybridized with O 2p states to yield a broad band. In contrast, the  $t_{2g}$  states in Co-doped ZnO are shallow and located above the O 2p valence band and so the hybridization becomes weak.

The total magnetic moments  $4.44$  and  $3.25\ \mu_B$  for Fe- and Co-doped ZnO come mostly from Fe ( $4.11\ \mu_B$ ) and Co ( $2.92\ \mu_B$ ) ions, respectively. These results suggest electron occupancies of  $d^6$  ( $\text{Fe}^{2+}$ ) and  $d^7$  ( $\text{Co}^{2+}$ ), respectively. Figure 3 provides the band structure of  $\text{Zn}_{0.9375}\text{Co}_{0.0625}\text{O}$  near  $E_F$ . Note that the size of circle represents the amount of Co 3d component in the wave function. It is seen that the rather flat majority spin Co 3d states are located by  $\sim 1.0\text{ eV}$  below the conduction band consisting of mainly Zn 4s states. The minority spin Co 3d states are located near and above  $E_F$  manifesting hybridization with the Zn 4s conduction band states. However, we do not expect that either Fe- or Co-

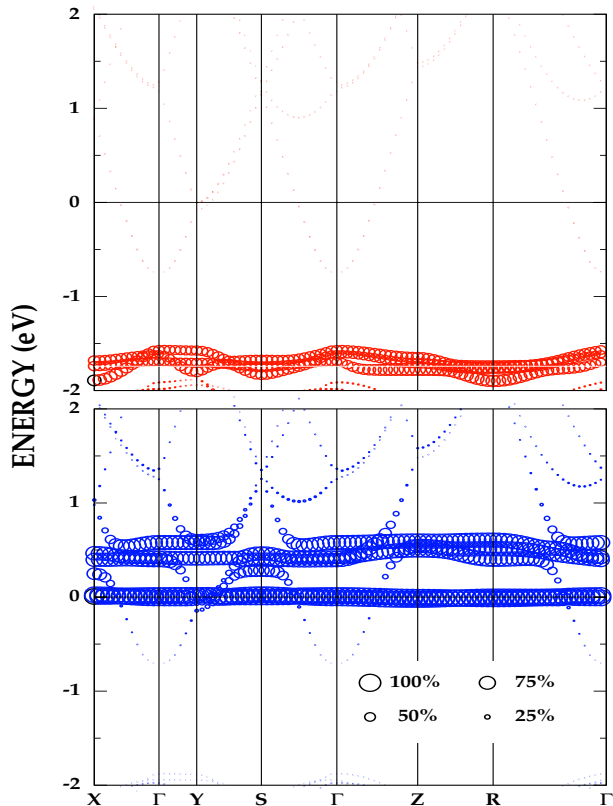


FIG. 3: Band structure of  $\text{Zn}_{0.9375}\text{Co}_{0.0625}\text{O}$  near the Fermi level (the upper panel for the majority and the lower for the minority spin band). The size of circle represents the amount of Co  $3d$  component in the wave function.

doped ZnO in nature has a stable metallic ferromagnetic ground state, as obtained above. The high DOSs at  $E_F$  for both Fe- and Co-doped ZnO would drive the possible structural instability or become reduced substantially by the Coulomb correlation interaction between TM  $3d$  electrons. Indeed, LSDA+ $U$  band calculation with  $U=5.0\text{eV}$  for Co  $3d$  electrons yields the insulating ground state for Co-doped ZnO, distinctly from the LSDA band results<sup>20</sup>.

### III. (Fe,Co) codoped ZnO

Now we have performed the LSDA band calculations for (Fe, Co) codoped ZnO:  $\text{Zn}_{0.875}(\text{Fe}_{0.5}\text{Co}_{0.5})_{0.125}\text{O}$ . We have examined magnetic properties of supercell by varying the separation between Fe and Co: 3.2499, 5.6055, and 6.4998 Å. 3.2499 Å corresponds to a nearest Fe-Co separation with Fe-O-Co configuration in the a-b plane of the orthorhombic supercell, while 5.6055 and 6.4998 Å to farther Fe-Co separations with Fe-O-Zn-O-Co configurations along the diagonal direction and in the a-b plane, respectively. Total energies are nearly the same among three cases: the shortest 3.2499 Å case has the lowest total energy by only  $\sim 3$  mRy. This result reflects that there will not be any noticeable TM clustering effect in the (Fe, Co) codoped ZnO. Further we have found that

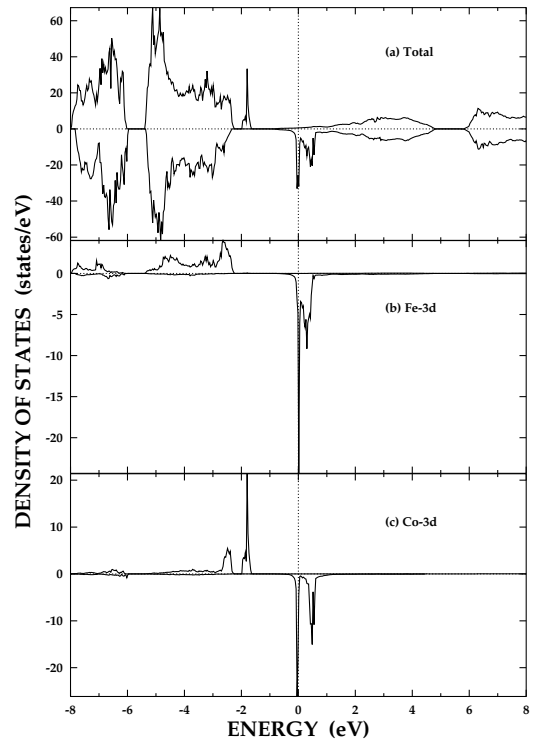


FIG. 4: The LSDA total and TM  $3d$  PLDOSs of  $\text{Zn}_{0.875}\text{Fe}_{0.0625}\text{Co}_{0.0625}\text{O}$ .

the FM configuration of Fe and Co spins are found to be slightly more stable than the antiferromagnetic (AFM) configuration for all three cases.

Figure 4 shows the LSDA DOS of  $\text{Zn}_{1-2x}\text{Fe}_x\text{Co}_x\text{O}$  ( $x = 0.0625$ ) for a Fe-Co separation of 5.6055 Å. The  $3d$  PLDOS in the codoped case looks as if it is just a simple sum of Fe and Co PLDOSs of Fig. 2. There is no indication of charge transfer between Fe and Co, and so  $\text{Fe}^{2+}$  and  $\text{Co}^{2+}$  valence configurations are retained in the (Fe, Co) codoped ZnO. Hence most properties are similar to each Fe- and Co-doped case, such as the degree of hybridization, nearly half-metallic nature, and the local magnetic moments. This suggests that the *double-exchange* mechanism<sup>21</sup> will not be effective in  $\text{Zn}_{1-2x}\text{Fe}_x\text{Co}_x\text{O}$ , because the kinetic-energy gain through the hopping of spin-polarized carriers between Fe and Co ions does not seem to occur. Thus to explain the observed FM ground state in  $\text{Zn}_{1-2x}\text{Fe}_x\text{Co}_x\text{O}$ , one needs to invoke another exchange mechanism between Fe and Co, such as the RKKY-type exchange interaction mediated by Zn  $4s$  carriers or conduction carriers induced by oxygen vacancies. However, one cannot rule out the formation of separated Fe or Co metallic clusters in  $\text{Zn}_{1-2x}\text{Fe}_x\text{Co}_x\text{O}$  which would exhibit the ferromagnetism. Also the possible formation of impurity phases such as spinel  $\text{CoFe}_2\text{O}_4$  is worthwhile to be checked carefully. These features remain to be resolved more in the experiments.

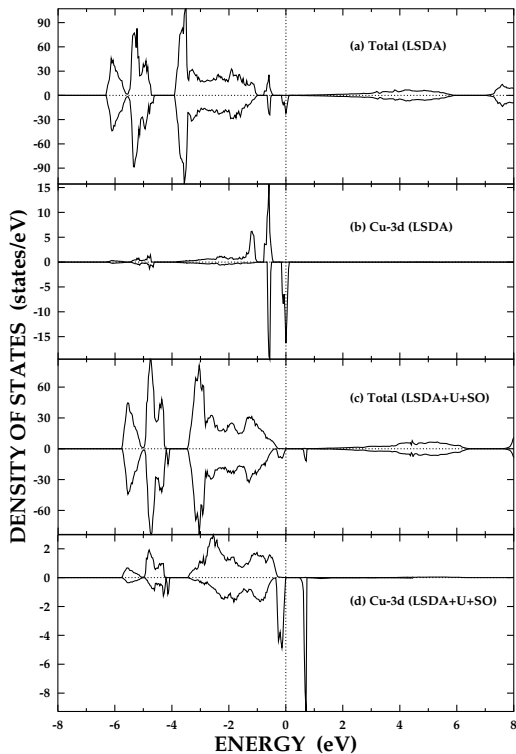


FIG. 5: The LSDA and LSDA+ $U$ +SO ( $U=3.0$  eV) total and Cu 3d PLDOSs for  $\text{Zn}_{0.9375}\text{Cu}_{0.0625}\text{O}$ .

#### IV. Cu-doped ZnO

Before discussing (Fe, Cu) codoped ZnO, we have examined electronic structure of Cu only doped ZnO:  $\text{Zn}_{0.9375}\text{Cu}_{0.0625}\text{O}$ . Interestingly, as shown in Fig. 5, we have obtained the stable FM and half-metallic ground state for Cu-doped ZnO in the LSDA. The total magnetic moment is  $1 \mu_B$  and the local moment of Cu is  $0.81 \mu_B$ , corresponding to the  $\text{Cu}^{2+}$  ( $d^9$ ) valence state. The Cu 3d PLDOS in Fig. 5(b) indicates that Cu has the DOS of an intermediate spin state. In contrast to Fe- or Co-doped case, the empty Cu 3d states are located in the gap region without the hybridization with the Zn 4s conduction band, and thus Cu 3d states are strongly localized. We presume that this would be the reason why the Cu solubility in ZnO is so low:  $\sim 1\%$  at most.

Since the Cu 3d states near  $E_F$  correspond to partially occupied atomic-like  $t_{2g}$  states, Cu ions would have large orbital magnetic moment. Indeed the LSDA+ $U$ +SO calculation yields the substantial orbital magnetic moment of  $1.05 \mu_B$  with the insulating electronic structure<sup>22</sup>. The large orbital moment arises from occupied minority spin  $t_{2g}$  states split by the Coulomb correlation and the spin-orbit interaction<sup>23</sup>. The orbital moment is polarized in parallel with the spin moment, and so the total magnetic moment amounts to  $1.85 \mu_B/\text{Cu}$ .

In general, an ion at the tetrahedral center with low spin  $d^9$  state would be Jahn-Teller active. In fact, there

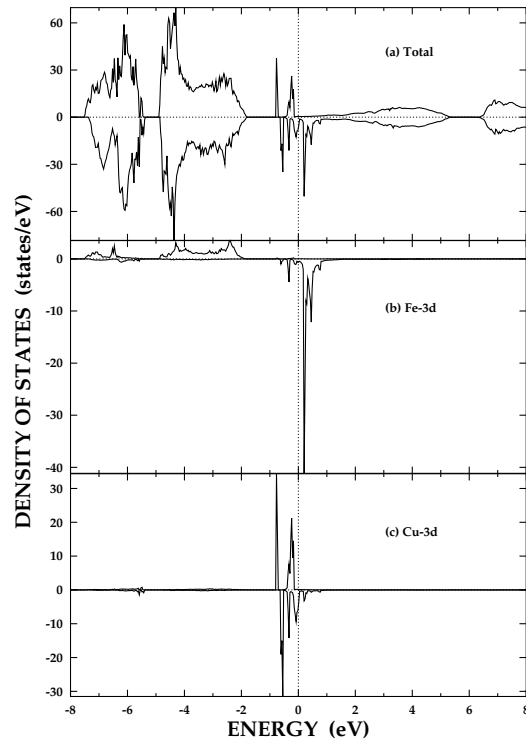


FIG. 6: The LSDA total and TM 3d PLDOSs for  $\text{Zn}_{0.875}\text{Fe}_{0.0625}\text{Cu}_{0.0625}\text{O}$ .

was a report that the account of the dynamical Jahn-Teller effect is necessary to explain the observed paramagnetic susceptibility for Cu-doped ZnO<sup>24</sup>. To examine the Jahn-Teller effect in Cu-doped ZnO, we have considered the local distortion of a tetrahedron around Cu by tilting oxygen ions at the corners. The oxygen ions are tilted by  $\sim 13^\circ$  toward the  $xy$ -plane with retaining Cu-O separations (here  $xyz$  coordinates represent the local principle axis). The LSDA band calculation for this system yields a more stable insulating ground state with enhanced spin magnetic moment of  $0.99 \mu_B/\text{Cu}$ . That is, due to the Jahn-Teller distortion, Cu 3d electrons become more localized and the system becomes insulating. The orbital moment in this case would be quenched due to the Jahn-Teller effect.

#### V. (Fe,Cu) codoped ZnO

As is done for (Fe, Co) codoped case, we have studied magnetic properties of (Fe, Cu) codoped  $\text{Zn}_{1-2x}\text{Fe}_x\text{Cu}_x\text{O}$  ( $x = 0.0625$ ) with varying the separation between Fe and Cu: 3.2499, 5.6055, and 6.4998 Å. For all three cases, the FM configurations of Fe and Cu spins are found to be more stable than the AFM configurations, as for the (Fe, Co) codoped case. In contrast to the (Fe, Co) codoped case, however, we have found that the shortest Fe-Cu configuration becomes much more stable with respect to

other two cases by  $\sim 30$  mRy. This total energy difference is very large when comparing with  $\sim 3$  mRy difference for the (Fe, Co) codoped case. This result indicates that Fe and Cu ions in (Fe, Cu) codoped ZnO have a tendency to form the Fe-O-Cu clusters. For 1 % Cu-doped  $\text{Zn}_{0.95}\text{Fe}_{0.05}\text{O}$  bulk sample, Han *et al.*<sup>13</sup> observed rather small saturated magnetic moment of  $0.75 \mu_B$  per Fe. This value corresponds to only about 1/5 of ideal  $\text{Fe}^{2+}$  local moment  $4 \mu_B$ . Incidentally, the value 1/5 is matched with Cu/Fe doping ratio, suggesting a possibility that the only Fe's forming the Fe-O-Cu clusters would give rise to the FM moment, that is, other Fe ions do not produce the long range FM order. As shown below, the FM ground state in (Fe, Cu) codoped ZnO can be understood based on the enhanced double-exchange-like interaction through the Fe-O-Cu clustering effect.

Figure 6 presents the LSDA DOS of  $\text{Zn}_{0.875}\text{Fe}_{0.0625}\text{Cu}_{0.0625}\text{O}$  for the shortest 3.2499 Å configuration. Above all, one can notice the strong hybridization between Fe and Cu 3d states. Further, it is clearly seen in Fig. 6(c) that some new states emerge in the Cu 3d minority spin PLDOS between  $e_g$  and  $t_{2g}$ . The new states have  $d_{xy}$ -like characters directing toward Fe ions<sup>25</sup>. Cu 3d PLDOS has a reduced exchange splitting, manifesting the DOS characteristic of the low spin state. This feature is different from other two configurations with larger Fe-Cu separation, which have an intermediate spin state as in Cu only doped ZnO. For all three cases, the hybridization between Cu 3d and the conduction band exists, which is again distinct from Cu only doped ZnO. Due to this hybridization, the conduction carriers of mostly Zn 4s states become reduced. Noteworthy from PLDOSs of Fig. 6 is that there occurs charge transfer from Fe to Cu, and accordingly Fe and Cu are likely to have nominal  $\text{Fe}^{3+}$  ( $d^5$ ) and  $\text{Cu}^{1+}$  ( $d^{10}$ ) configurations, respectively. As a result, the electron occupancy at Cu site increases, and so Cu has the reduced spin magnetic moment of  $0.51 \mu_B$  as compared to  $0.81 \mu_B$  in Cu only doped ZnO. This feature explains the experimental result of the reduced number of carriers in (Fe, Cu) codoped ZnO with respect to that in Fe only doped ZnO<sup>13</sup>. The charge transfer from Fe

to Cu is expected to disturb the Jahn-Teller distortion at Cu sites and concomitantly make a system metallic. Further, it will cause the mixed-valent occupancies for Fe ( $\text{Fe}^{2+}$ - $\text{Fe}^{3+}$ ) and Cu ( $\text{Cu}^{2+}$ - $\text{Cu}^{1+}$ ) ions, and the consequent double-exchange-like interaction is expected to induce the ferromagnetism in (Fe, Cu) codoped ZnO.

## VI. CONCLUSION

We have investigated electronic structures of (Fe, Co) and (Fe, Cu) codoped ZnO together with those of Fe-, Co-, and Cu-doped ZnO. We have also explored origins of observed ferromagnetism in (Fe, Co) and (Fe, Cu) codoped ZnO. The single TM-doped systems would not have stable metallic ferromagnetic ground states, due to large Coulomb correlation or other structural instability effects in Fe- and Co-doped ZnO and the Jahn-Teller effect in Cu-doped ZnO, respectively. For (Fe, Co) codoped ZnO, we have found no indication of charge transfer between Fe and Co, suggesting that the double-exchange mechanism will not be effective for the observed ferromagnetism in (Fe, Co) codoped ZnO. Therefore one needs to invoke another exchange mechanism between Fe and Co, or the possible formation of impurity phases is to be checked carefully. In contrast, for (Fe, Cu) codoped ZnO, there is a tendency to form the Fe-O-Cu clusters and so to give rise to charge transfer from Fe to Cu ion. This tendency causes the mixed-valent occupancies between Fe and Cu, and accordingly the double-exchange-like interaction is expected to induce the ferromagnetism in (Fe, Cu) codoped ZnO. The FM and nearly half-metallic ground state is obtained for (Fe, Cu) codoped ZnO.

## Acknowledgments

This work was supported by the KOSEF through the eSSC at POSTECH and in part by the KRF (KRF-2002-070-C00038). Helpful discussions with Y. H. Jeong and S. J. Han are greatly appreciated.

---

<sup>1</sup> S. A. Wolf, D. D. Awschalom, R. A. Buhrman, J. M. Daughton, S. von Molnar, M. L. Roukes, A. Y. Chtchelkanova, and D. M. Treger, *Science* **294**, 1488 (2001).  
<sup>2</sup> J. K. Furdyna and J. Kossut, *DMSs, Semiconductor and Semimetals* **25**, Academic Press, New York, (1988).  
<sup>3</sup> H. Ohno, A. Shen, F. Matsukura, A. Oiwa, A. Endo, S. Katsumoto, and Y. Iye, *Appl. Phys. Lett.* **69**, 363 (1996).  
<sup>4</sup> T. Dietl, H. Ohno, F. Matsukura, J. Cibert, and D. Ferrand, *Science* **287**, 1019 (2000).  
<sup>5</sup> K. Sato and H. K. Yoshida, *Semicond. Sci. Technol.* **17**, 367 (2002).  
<sup>6</sup> G. A. Medvedkin, T. Ishibashi, T. Nishi, K. Hayata, Y. Hasegawa, and K. Sato, *Jpn. J. Appl. Phys.* **39**, L949 (2000).

<sup>7</sup> Y. Matsumoto, M. Murakami, T. Shono, T. Hasegawa, T. Fukumura, M. Kawasaki, P. Ahmet, T. Chikyow, S. Koshihara, and H. Koinuma, *Science* **291**, 854 (2001).  
<sup>8</sup> K. Ando, H. Saito, Z. Jin, T. Fukumura, M. Kawasaki, Y. Matsumoto, and H. Koinuma, *Appl. Phys. Lett.* **78**, 2700 (2001).  
<sup>9</sup> S. Cho, S. Choi, G.-B. Cha, S. C. Hong, Y. Kim, Y.-J. Zhao, A. J. Freeman, J. B. Ketterson, B. J. Kim, Y. C. Kim, B.-C. Choi, *Phys. Rev. Lett.* **88**, 257203 (2002)  
<sup>10</sup> Z. Jin, T. Fukumura, M. Kawasaki, K. Ando, H. Saito, T. Sekiguchi, Y. Z. Yoo, M. Murakami, Y. Matsumoto, T. Hasegawa, and H. Koinuma, *Appl. Phys. Lett.* **78**, 3824 (2001).  
<sup>11</sup> K. Ueda, H. Tabata, and T. Kawai, *Appl. Phys. Lett.* **79**,

- 988 (2001).
- <sup>12</sup> Y. M. Cho, W. K. Choo, H. Kim, D. Kim, and Y. Ihm, Appl. Phys. Lett. **80**, 3358 (2002).
- <sup>13</sup> S. -J. Han, J. W. Song, C.-H. Yang, S. H. Park, J.-H. Park, Y. H. Jeong, and K. W. Rhie, Appl. Phys. Lett. **81**, 4212 (2002).
- <sup>14</sup> S. K. Kwon and B. I. Min, Phys. Rev. Lett. **84**, 3970 (2000).
- <sup>15</sup> P. Schröder, P. Kruger, and J. Pollmann, Phys. Rev. B **47**, 6971 (1993).
- <sup>16</sup> M. Oshikiri and F. Aryasetiawan, J. Phys. Soc. Japan, **69**, 2113 (2000).
- <sup>17</sup> M. Usuda, N. Hamada, T. Kotani, and M. van Schilfgaarde, Phys. Rev. B **66**, 125101 (2002).
- <sup>18</sup> M. Ruckh, D. Schmid, and H. W. Schock, J. Appl. Phys. **76**, 5945 (1994).
- <sup>19</sup> Since the Zn *3d* bands in the LSDA are located still deep in energy, the effects of the Zn *3d* bands on the magnetic properties of TM doped ZnO will be minor.
- <sup>20</sup> For Fe-doped ZnO, the LSDA+*U* band calculation with  $U = 5.0$  eV does not yield the converged results, probably because of too high DOS at  $E_F$ . With  $U=9.0$ eV, we can obtain the converged insulating ground state.
- <sup>21</sup> C. Zener, Phys. Rev. B **82**, 403 (1951).
- <sup>22</sup> We employed parameter values of  $U=3.0$  eV and  $J=0.87$  eV ( $J$ : exchange parameter) for Cu *3d* electrons.
- <sup>23</sup> M. S. Park, S. K. Kwon, and B. I. Min, Phys. Rev. B **65**, 161201(R) (2002).
- <sup>24</sup> W. H. Brumage, C. F. Dorman, and C. R. Quade, Phys. Rev. B **63**, 104411 (2001).
- <sup>25</sup> Here too *xyz* coordinates represent the local principal axis.